ISSN 1070-3632, Russian Journal of General Chemistry, 2014, Vol. 84, No. 8, pp. 1593–1598. © Pleiades Publishing, Ltd., 2014.
Original Russian Text © E.A. Katlenok, A.A. Zolotarev, K.P. Balashev, 2014, published in Zhurnal Obshchei Khimii, 2014, Vol. 84, No. 8, pp. 1372–1377.

Binuclear Complexes of Pt(II) with Platinated 2-Phenylbenzothiazole and Bridged Derivatives of Pyridin- and Benzothiazol-2-thiols

E. A. Katlenok[a], A. A. Zolotarev[b], and K. P. Balashev[a]

[a] *Herzen State Pedagogical University of Russia, nab. reki Moiki 48, St. Petersburg, 191186 Russia*
e-mail: balashevk@mail.ru

[b] *St. Petersburg State University, St. Petersburg, Russia*

Received April 8, 2014

Abstract—Binuclear complexes of Pt(II) cycloplatinated with 2-phenylbenzothiazole and bridging ligands have been shown to contain the Pt–Pt bond. The complexes have been studied by X-ray diffraction, ^{1}H NMR and electronic absorption spectroscopy, and electrochemical methods. The complexes *cis*-$N_{(bt)}$,S-isomers with antisymmetric positions of the cyclometalated and the bridging ligands have been detected in the crystals as well as in the solutions. The low-wavelength absorption and luminescence of the complexes have been assigned to the metal–metal–ligand charge transfer. The two-electron oxidation and reduction waves in the voltamperograms are associated with the metal- and the ligand-centered processes, respectively.

Keywords: binuclear complex, platinum, cyclometalated complex, structure, absorption spectrum, emission spectrum, cyclic voltammetry

DOI: 10.1134/S107036321408026X

Due to strong room-temperature phosphorescence in solid state and in solution, cyclometalated complexes of Ir(III) and Pt(II) with heterocyclic ligands are promising for development of triplet actuators of organic light-emitting systems, photocatalysts, optical chemosensors, and optical biological labels [1–5]. Planar structure of cyclometalated Pt(II) complexes enables their association via π–π- or d_{z^2}–d_{z^2} interactions of metal ions and ligands to alter the nature and energy of HOMO and LUMO of the complex reflected in their optical and electrochemical properties [6, 7]. When Pt–Pt bond is formed due to overlap of the d_{z^2}–d_{z^2} metal ions orbitals, the σ* orbital becomes the complex HOMO (Fig. 1), explaining red phosphorescence and possibility to undergo two-electron oxidation into Pt(III) complexes [7–10].

In this work we discuss structural, spectroscopic, and electrochemical studies of binuclear Pt(II) complexes, $[Pt(bt)(\mu\text{-pyt})]_2$ and $[Pt(bt)(\mu\text{-mbt})]_2$, containing cycloplatinated 2-phenylbenzothiazole {Pt(bt)} as peripheral ligands and pyridin-2-thiolate (pyt^-) or benzothiazol-2-thiolate (mbt^-) as bridging ligands (Scheme 1).

X-ray diffraction studies of the complexes monocrystals (Table 1; Figs. 2 and 3) revealed the presence of the *cis*-$N_{(bt)}$,S isomers of the $[Pt(bt)(\mu\text{-mbt})]_2$ complex and the $[Pt(bt)(\mu\text{-pyt})]_2\cdot CH_2Cl_2$ solvate with antisymmetric positioning of two cyclometalated and two bridging ligands in the crystal form. The distance between Cl of dichloromethane and H of benzothiazole of the cyclometalated ligand in $[Pt(bt)(\mu\text{-pyt})]_2\cdot CH_2Cl_2$

Scheme 1.

{Pt(bt)} = 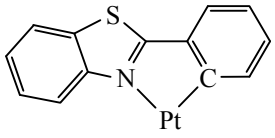

{Pt(μ-pyt)} = 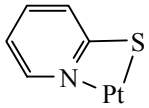

{Pt(μ-mbt)} = 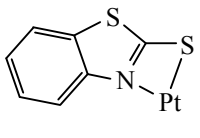

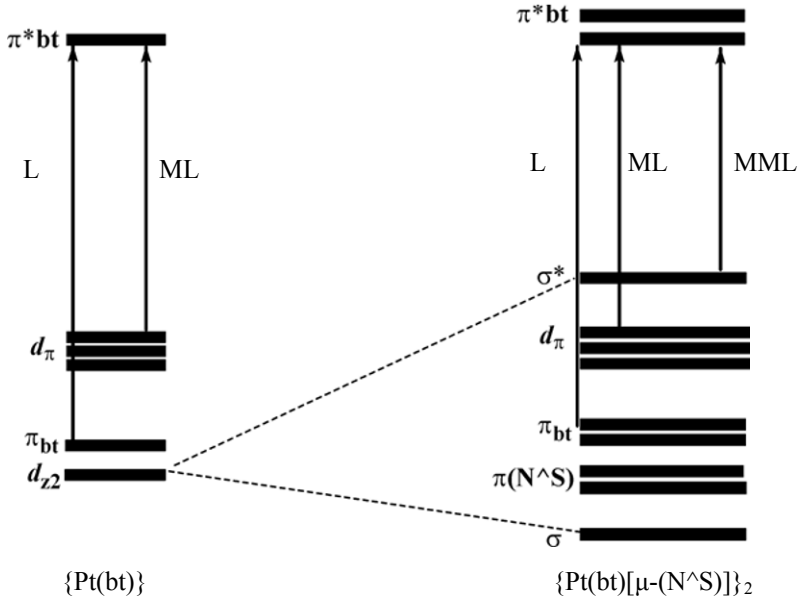

Fig. 1. Qualitative molecular orbitals diagram of binuclear Pt(II) complexes containing the Pt–Pt bond. (L) intraligand transition; (ML) metal-ligand charge transfer; (MML) metal-metal-ligand charge transfer.

Table 1. X-ray diffraction data and parameters of the complexes structure refinement

Parameter	$[Pt(bt)(\mu\text{-pyt})]_2 \cdot CH_2Cl_2$	$[Pt(bt)(\mu\text{-mbt})]_2$
Formula	$C_{37}H_{26}N_4Pt_2S_4Cl_2$	$C_{40}H_{24}N_4Pt_2S_6$
Molar mass, g/mol	1115.94	1143.17
Crystal system	Triclinic	Triclinic
Space group	*P*-1	*P*-1
Unit cell geometry	*a* 11.3370(7), *b* 12.7070(8), *c* 13.5951(8) Å; α 67.987(5), β 89.028(5), γ 76.762(5)°; *V* 1771.16(18) Å^3; *Z* 2	*a* 10.2790(3), *b* 11.5964(4), *c* 16.124(5) Å; α 110.916(3), β 95.659(2), γ 90.053(2)°; *V* 1785.04(9) Å^3; *Z* 2
d_{calc}, g/mL	2.092	2.127
μ, mm^{-1}	8.311	8.218
F(000)	1060.0	1088.0
Crystal size, mm	0.22×0.17×0.10	0.21×0.17×0.08
Irradiation	MoK_α (λ 0.71073)	MoK_α (λ 0.71073)
2θ range	(5.64–55)°	(5.06–55)°
Indexes range	$-14 \le h \le 14$, $-16 \le k \le 16$, $-17 \le l \le 17$	$-13 \le h \le 13$, $-14 \le k \le 15$, $-20 \le l \le 20$
Number of reflections	17635	26122
Independent reflections	7844 [R_{int} 0.0421, R_{sigma} 0.0637]	8043 [R_{int} 0.0389, R_{sigma} 0.0488]
GOF	1.054	1.057
R factors [$\|F_o\| \ge 4\sigma_F$]	R_1 0.0378, wR_2 0.0810	R_1 0.0277, wR_2 0.0544
R factors [all data]	R_1 0.0516, wR_2 0.0891	R_1 0.0392, wR_2 0.0591
ρ_{min}, ρ_{max}, e/Å^{-3}	2.81, –2.82	2.15, –0.98

$R_1 = \Sigma||F_0| - |F_c||/\Sigma|F_0|$; $wR_2 = \{\Sigma[w(F_0^2 - F_c^2)^2]/\Sigma[w(F_0^2)^2]\}^{1/2}$;
$w = 1/[\sigma^2(F_0^2) + (aP)^2 + bP]$, where $P = (F_0^2 + 2F_c^2)/3$; $s = \{\Sigma[w(F_0^2 - F_c^2)]/(n-p)\}^{1/2}$,
(*n*) number of reflections, (*p*) number of refined parameters

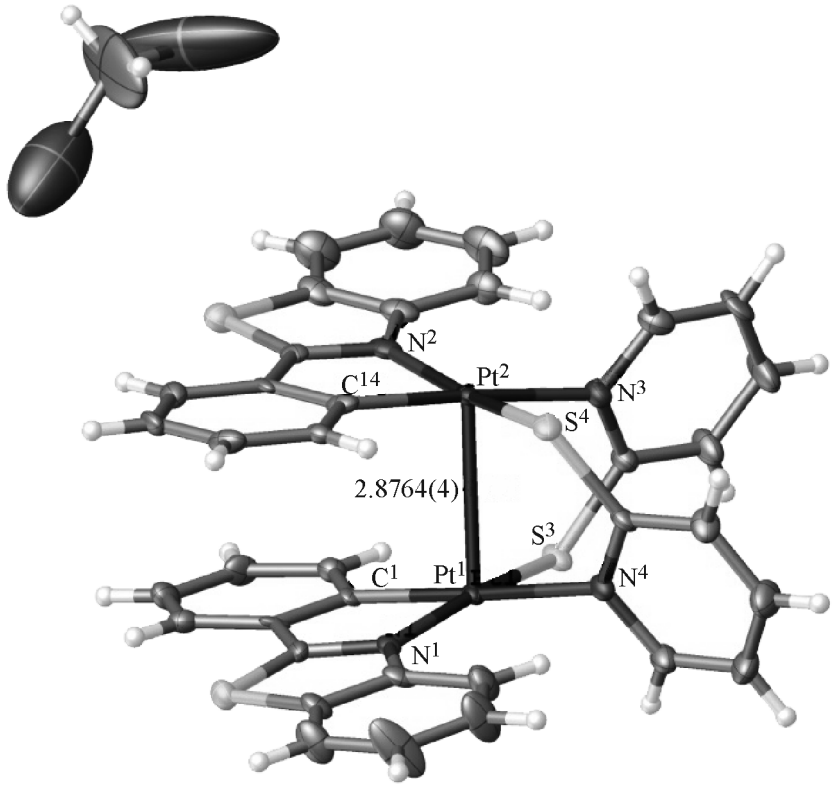

Fig. 2. General view of the $[Pt(bt)(\mu\text{-pyt})]_2 \cdot CH_2Cl_2$ molecule.

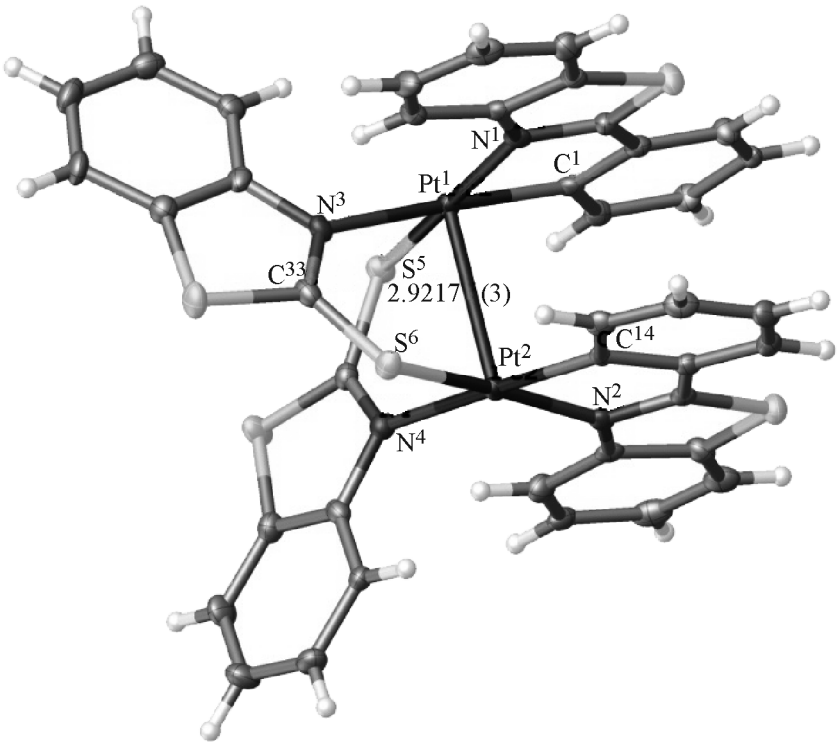

Fig. 3. General view of the $[Pt(bt)(\mu\text{-mbt})]_2$ molecule.

Table 2. Bond lengths, bond and torsion angles in the studied complexes

d, Å	$[Pt^{II}(bt)(\mu\text{-pyt})]_2 \cdot CH_2Cl_2$		$[Pt^{II}(bt)(\mu\text{-mbt})]_2$	
Pt–Pt	2.88		2.92	
Pt–C_{bt}	2.02	2.01	2.00	
Pt–N_{bt}	2.09	2.06	2.07	
Pt–$N_{N\wedge S}$	2.14	2.13	2.14	
Pt–$S_{N\wedge S}$	2.28	2.27	2.28	2.29
Angle, deg	$[Pt^{II}(bt)(\mu\text{-pyt})]_2 \cdot CH_2Cl_2$		$[Pt^{II}(bt)(\mu\text{-mbt})]_2$	
$N_{bt}PtC_{bt}$	80.7	81.1	80.8	80.6
$N_{bt}PtN_{N\wedge S}$	98.2	97.9	98.8	98.4
$N_{N\wedge S}PtS_{N\wedge S}$	87.8	88.0	86.3	87.6
$S_{N\wedge S}PtC_{bt}$	93.6	93.5	94.2	93.4
$PtPtN_{bt}C_{bt}$	88.9	84.7	87.2	91.3
$PtPtC_{bt}C_{bt}$	72.6	76.2	84.8	82.9
$PtPtN_{N\wedge S}C_{N\wedge S}$	25.2	26.9	17.1	17.5

was 3.23 Å, thus confirming formation of inter-molecular hydrogen bond.

The distance between platinum atoms (2.88–2.92 Å, Table 2) in the complexes as compared with twice van der Waals radius of Pt (4.58 Å [11]) confirmed formation of the Pt–Pt chemical bond in the binuclear complexes. Change of the bridging ligand nature resulted in the Pt–Pt length difference of only 0.04 Å.

The bond lengths and bond angles (Table 2) of the metal complex components of the binuclear Pt(II) complexes were different. However, sum of bond angles at Pt centers and N_{bt}, C_{bt} (cyclometalated ligand), $N_{N\wedge S}$, $S_{N\wedge S}$ (bridging ligand) donor centers was of 360.2°±0.2°, thus pointing at planar structure of the complexes coordination node.

A special feature of the binuclear complexes was almost parallel (Δ = 8°±4°) positioning of pair of antisymmetric cyclometalated ligands at the distance of 3.5–3.8 Å (Figs. 2 and 3). That enabled the π–π interaction and the mutual anisotropic influence of circular currents of phenyl and benzothiazole parts of the cyclometalated ligands, resulting in the upfield shift of their ^{1}H NMR signals. In contrast to the cyclometalated ligands (almost coinciding the coordinate planes), the planes of pyridine and benzothiazole parts of the bridging ligands were rotated by 83°±4° with respect to coordinate planes.

^{1}H NMR spectra of the complexes demonstrated that their molecular structure typical of the crystal was preserved in their solutions in $CDCl_3$. In particular, pairs of the cyclometalated and the bridging ligands were magnetically equivalent, and the protons signals were shifted upfield (Δδ of –0.3 to –1.2 ppm) in the case of cyclometalated ligands and downfield (Δδ = 0.3 to 1.3 ppm) in the case of bridging ligands.

Being in line with the qualitative diagram of molecular orbitals (Fig. 1) and data on the previously studied cyclometalated Pt(II) complexes containing the Pt–Pt bond [7–10], electronic absorption spectra of the $[Pt(bt)(\mu\text{-pyt})]_2$ and $[Pt(bt)(\mu\text{-mbt})]_2$ complexes contained the bands assigned to the following transitions: π–π* intraligand optical transition (λ < 330 nm), d–π^*_{bt} metal–ligand charge transfer (λ ≈380 nm), and $\sigma^*_{Pt^{II}}$–π^*_{bt} transition between HOMO and LUMO of the complexes (Table 3, Fig. 4; metal–metal–ligand charge transfer, λ = 425–540 nm). Photoexitation of the complexes solutions in dichloromethane resulted in red phosphorescence (emission bands with maximums at 678 and 694 nm were observed, their half-width being of about 2600 cm^{-1}). The excitation spectra were in line with the complexes absorption spectra; that confirmed the long-wavelength absorption band assignment to the spin-forbidden $\sigma^*_{Pt^{II}}$–π^*_{bt} transition (metal–metal–ligand charge transfer).

Voltamperograms of the complexes oxidation revealed irreversible two-electron wave corresponding

Table 3. Optical and electrochemical parameters of the studied complexes

Compound	λ_{max}, nm (ε × 10^3 L mol^{-1} cm^{-1})[a]	Phosphorescence[a]		Potential[b]	
		λ^{em}_{max}, nm (τ, μs)	λ^{ex}_{max}, nm	E^{ox}_p, V	$E^{red}_{1/2}$, V
$[Pt(bt)(\mu\text{-pyt})]_2$	313(40.0), 330 sh (32), 380 (16.8), 434 sh (6.0), 480 (3.55), 505 (3.40), 515 sh (3.2), 540 sh (2.5)	694 (6)	388, 425, 450 sh, 486, 530	0.04	–2.27
$[Pt(bt)(\mu\text{-mbt})]_2$	314 (52.5), 337 sh (37), 381 (15.1), 425 sh (5.8), 476 (3.41), 507 (3.18), 540 sh (1.7)	678 (5)	383, 423, 446 sh, 486, 530	0.45	–1.97

[a] CH_2Cl_2. [b] $C_6H_5CH_3$–CH_3CN, 1 : 1.

to elimination of electrons from the $\sigma^*_{Pt^{II}}$-HOMO and formation of binuclear Pt(III) complexes.

$$[Pt^{II}(bt)(\mu\text{-}N\text{^}S)]_2 - 2e^- \rightarrow \{Pt^{III}\}.$$

Extension of the Pt–Pt bond in the $[Pt(bt)(\mu\text{-mbt})]_2$ complex as compared to that in the $[Pt(bt)(\mu\text{-pyt})]_2$ complex was reflected in the oxidation potential shift by 0.41 V towards anodic range.

The reversible two-electron reduction waves of the complexes at –1.97 and –2.27 V were assigned to the ligand-centered reduction of the cyclometalated ligands.

$$[Pt^{II}(bt)(\mu\text{-}N\text{^}S)]_2 + 2e^- \rightleftarrows [Pt^{II}(bt^-)(\mu\text{-}N\text{^}S)]_2.$$

To conclude, the studied complexes revealed relatively stable crystal structure preserved in the dichloromethane solution. The main feature of the complexes was the presence of the Pt–Pt chemical bond leading to formation of the σ* HOMO contributing to the complexes optical and electro-chemical processes.

EXPERIMENTAL

^{1}H NMR spectra of the complexes solutions in $CDCl_3$ were recorded using the JNM-ECX400A spectrometer. Electronic absorption spectra of the solutions in CH_2Cl_2 were registered using the SF-2000 spectrophotometer. Phosphorescence excitation and emission spectra of the solutions in CH_2Cl_2 were recorded using the Flyuorat-02 Panorama spectrofluorimeter.

Voltamperograms were obtained using the IPC-PRO device equipped with the divided cell (working glassy carbon electrode, auxiliary Pt electrode and Ag reference electrode) in the presence of 0.1 mol/L of $[NBu_4]PF_6$ in $C_6H_5CH_3$–CH_3CN, (1 : 1). The peaks potentials were reported as referenced to the ferrocenium/ferrocene redox pair at 100 mV/s.

X-ray diffraction studies were performed at 100 K using the Agilent Technologies Excalibur Eos monocrystal diffractometer equipped with flat detector of the reflected X-rays (charge-coupled device). The crystallographic data and refinement parameters are collected in Table 1. The unit cell parameters were refined taking advantage of the least squares procedure. The structures were solved by direct method and refined by full-matrix least squares procedure in anisotropic approximation (SHELXL [12] software of the OLEX2 [13] software package). Absorption was corrected for using the CrysAlisPro [14] software package. Hydrogen atoms were included in the refinement with fixed positions and temperature parameters. The X-ray data were deposited at the Cambridge Crystallographic Data Centre (CCDC 988517 and 993566).

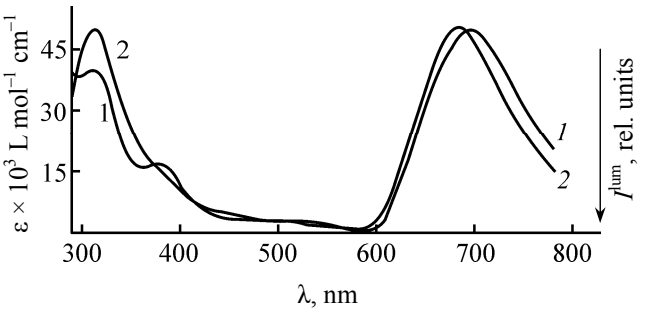

Fig. 4. Electronic absorption and luminescence spectra of the $[Pt(bt)(\mu\text{-pyt})]_2$ (*1*) and $[Pt(bt)(\mu\text{-mbt})]_2$ (*2*) complexes in CH_2Cl_2.

The $[Pt(bt)(\mu\text{-mbt})]_2$ and $[Pt(bt)(\mu\text{-pyt})]_2$ complexes were prepared as described elsewhere [7, 15].

Bis[(μ-2-thiopyridinato)(2-phenyl-3-ido)benzothiazolplatinum] $[Pt(bt)(\mu\text{-pyt})]_2$. ^{1}H NMR spectrum ($CDCl_3$), δ, ppm (*J*, Hz): 8.85 d (2H, $^3J_{HH}$ 5.5), 7.73 d (2H, $^3J_{HH}$ 7.9), 7.45 d (2H, $^3J_{HH}$ 8.3), 7.29 d.d (2H, $^3J_{HH}$ 4.1, 7.3), 7.28 d (2H, $^3J_{HH}$ 8.1), 7.19 t. d (2H, $^3J_{HH}$ 7.8, $^4J_{HH}$ 1.4), 7.12 d.d (2H, $^3J_{HH}$ 8.1, 7.5), 7.04 d (2H, $^3J_{HH}$ 7.7), 6.86 d.d (2H, $^3J_{HH}$ 6.0, 6.9), 6.81 t (2H, $^3J_{HH}$ 7.5), 6.38 d (2H, $^3J_{HH}$ 8.7), 6.35 d.d (2H, ^3J 8.7, 7.6).

Bis[(μ-2-thiobenzothiazolato)(2-phenyl-3-ido)-benzothiazolplatinum] $[Pt(bt)(\mu\text{-mbt})]_2$. ^{1}H NMR spectrum ($CDCl_3$), δ, ppm (*J*, Hz): 8.71 d (2H, $^3J_{HH}$ 8.2), 7.59 d (4H, $^3J_{HH}$ 7.7), 7.43 d (2H, $^3J_{HH}$ 7.7), 7.29–7.20 m (4H), 7.23 m (2H), 7.10 m (2H), 7.11 d (2H, $^3J_{HH}$ 7.5), 7.09 m (2H^5), 6.69 t (2H, $^3J_{HH}$ 7.4), 6.57 d (2H, ^3J 8.4), 6.21 t (2H, $^3J_{HH}$ 7.6).

REFERENCES

1. Williams, J.A.G., Develay, S., Rochester, D.L., and Murphy, L., *Coord. Chem. Rev*., 2008, vol. 252, nos. 23–24, p. 2596. DOI: 10.1016/j.ccr.2008.03.014.
2. You, Y. and Nam, W., *Chem. Soc. Rev*., 2012, vol. 41, no. 21, p. 7061. DOI: 10.1039/c2cs35171d.
3. Goldsmith, G.I., Hudson, W.R., Lowry, M.S., Anderson, T.H., and Bernhard, S., *J. Am. Chem. Soc*., 2005, no. 20, p. 7502. DOI: 10.1021/ja0427101.
4. Rogers, C.W. and Wolf, M.O., *Coord. Chem. Rev*., 2002, vols. 233–234, p. 341. DOI: 10.1016/s0010-8545-(02)00023-1.

5. Yang, Y., Zhao, Q., Feng, W., and Li F., *Chem. Rev*., 2013, vol. 113, no. 1, p. 192. DOI: 10.1021/cr2004103.
6. Bercaw, J.E., Durell, A.C., Gray, H.B., Green, J.C., Hazari, N., Labinger, J.A., and Winkler, J.R., *Inorg. Chem*., 2010, vol. 49, no. 4, p. 1801. DOI: 10.1021/ic902189g.
7. Aoki, R., Kobayashi, A., Chang, H.-C., and Kato, M., *Bull. Chem. Soc. Japan*, 2011, vol. 84, no. 2, p. 218. DOI: 10.1246/bcsj.2010.03.04.
8. Katlenok, K.E. and Balashev, K.P., *Optics and Spectroscopy*, 2014, vol. 116, no. 1, p. 100. DOI: 10.7868/S0030400X13120096.
9. Chakraborty, A., Deaton, J.C., Haefele, A., and Castellano, F.N., *Organometallics,* 2013, vol. 32, no. 14, p. 3819. DOI: 10.1021/om400276v.
10. Sicilia, V., Fornies, J., Casas, J.M., Martin, A., Lopez, J.A., Larraz, C., Borja, P., Ovejero, C., Tordera, D., and Bolink, H., *Inorg. Chem*., 2012, vol. 51, no. 6, p. 3427. DOI: 10.1021/ic201910t.
11. Alvarez, S., *Dalton Trans*., 2013, vol. 42, p. 8617. DOI: 10.1039/c3dt50599e.
12. Sheldrick, G.M., *Acta Cryst. (A),* 2008, vol. 64, no. 1, p. 112. DOI: 10.1107/S0108787307043930.
13. Dolomanov, O.V., Bourhis, L.J., Gildea, R.J., Howard, J.A.K., and Puschmann, H., *J. Appl. Cryst*., 2009, vol. 42, no. 2, p. 339. DOI: 10.1107/S0021889808042726.
14. *CrysAlisPro, Agilent Technologies*, Ver. 1.171.36.20 (release 27-06-2012).
15. Katlenok, K.E. and Balashev, K.P., *Russ. J. Gen. Chem*., 2014, vol. 84, no. 4, p. 791. DOI: 10.1134/S107036321404032X.